Discovery of Different Types of Inhibition between the Human and *Thermotoga maritima* α-Fucosidases by Fuconojirimycin-Based Derivatives†

Ching-Wen Ho,‡ Yu-Nong Lin,‡,§ Chuan-Fa Chang,‡ Shiou-Ting Li,‡ Ying-Ta Wu,‡ Chung-Yi Wu,‡ Chiung-Fang Chang,‡,§ Sheng-Wen Liu,|| Yaw-Kuen Li,|| and Chun-Hung Lin*,‡,§

Institute of Biological Chemistry and Genomics Research Center, Academia Sinica, No. 128, Academia Road Section 2, Nan-Kang, Taipei 11529, Taiwan, Institute of Biochemical Sciences, National Taiwan University, Taipei 10617, Taiwan, and Department of Applied Chemistry, National Chiao-Tung University, Hsin-Chu 30010, Taiwan

Received December 16, 2005; Revised Manuscript Received February 28, 2006

ABSTRACT: An efficient method for examining the selectivity of inhibitors on two α-fucosidases, one from *Thermotoga maritima* and the other from human, was established. The X-ray crystal structure of the former enzyme makes possible the homology modeling of the human α-fucosidase, indicating the major difference between both enzymes in the periphery of the catalytic site. To investigate the difference at the molecular level, a variety of fuconojirimycin (FNJ) derivatives with substitution at C1, C2, C6, or N were rapidly prepared in microplates and screened without purification for the inhibition activities of the two α-fucosidases. Among the molecules that were tested, only the substitution at C1 can significantly enhance the inhibitory potency, in contrast to the control (no substitution) and compounds with substitution at other positions. The majority of C1-substituted FNJs were found to be slow tight-binding inhibitors of the *Thermotoga* enzyme, while acting as the reversible inhibitors of the human fucosidase. The best inhibitor exhibited 13700-fold difference in affinity between the two enzymes, which was attributed to the dissimilar aglycon binding site. Further investigations were carried out, including site-directed mutagenesis, the comparison of K_i values among the wild type and mutants, and the intrinsic fluorescence change upon inhibitor titration, all supporting the idea that Tyr64 and Tyr267 of the *Thermotoga* α-fucosidase are critically involved in closely interacting with the aglycon of inhibitors. The increased level of contact thus induced conformational change, leading to the observed slow tight-binding inhibition.

During the development of enzyme inhibitors for drug discovery, selectivity is always a primary concern in addition to the pursuit of optimized inhibitory potency. In other words, desired molecules may simultaneously interact with several similar enzymes and thus cause possible side effects at the stage of *in vivo* or animal studies. The natural product swainsonine, for instance, has been known for its potent inhibition against Golgi α-mannosidase II (*1*−*4*) due to its five-membered ring resembling a flattened oxocarbenium transition state. By blocking the mannosidase activity, this indolidine alkaloid effectively shuts down the carbohydrate processing pathway prior to the initiation of the β1,6-GlcNAc-linked branch, which effectively inhibits tumor cell metastasis, decreases solid tumor growth in mice, and enhances the cellular immune response (*5*, *6*). Nonetheless, the inhibition of a related catabolic α-mannosidase in lysosomes makes its clinical use less desirable (*7*−*9*). Another example is nitric oxide synthases (NOSs)[1] that produce nitric oxide under a variety of physiological and pathophysiological conditions. Three distinct isoforms are termed endothelial NOS (eNOS), inducible NOS (iNOS), and neuronal NOS (nNOS) (*10*). Selective inhibition of iNOS may be beneficial in treating various forms of shock (*11*, *12*) and inflammation (*13*, *14*), while inhibition of nNOS likely protects against neuroinjury (*15*, *16*). As a consequence, identifying significant differences among similar enzymes or isoenzymes represents a crucial challenge.

Fucose-containing carbohydrates are often involved in a number of important physiological activities (*17*−*20*), which brings more attention to some specific α-fucosidases (*19*, *21*). Several pathogenic events, including inflammation (*18*), cancer (*21*, *22*), and cystic fibrosis (*23*, *24*), have been indicated in association with an abnormal distribution of α-fucosidases. The human α-fucosidase has been shown to be a diagnostic serum marker for the early detection of hepatocellular and colorectal carcinomas (*21*, *22*, *25*). In this report, a simple and efficient method for examining the difference between two α-fucosidases, one from *Thermotoga maritima* (designated TmF) and the other from human (HuF), has been developed. Unlike any other prokaryotic α-fucosidases, the *Thermotoga* α-fucosidase is closely related to those from the animal kingdom (*26*). Therefore, the former

† This work was supported by the National Science Council (NSC-94-2113-M-001-028 to C.-H.L.) and Academia Sinica, Taiwan.

* To whom correspondence should be addressed. Phone: +886-2-27890110. Fax: +886-2-2651-4705. E-mail: chunhung@gate.sinica.edu.tw.

‡ Academia Sinica.

§ National Taiwan University.

|| National Chiao-Tung University.

[1] Abbreviations: NOSs, nitric oxide synthases; eNOS, endothelial NOS; iNOS, inducible NOS; nNOS, neuronal NOS; TmF, *T. maritima* α-fucosidase; HuF, human α-fucosidase; FNJ, fuconojirimycin; HBTU, (1*H*-benzotriazol-1-yl)-1,1,3,3-tetramethyluronium hexafluorophosphate; DIEA, diisopropyl ethylamine.

10.1021/bi052559n CCC: $33.50
Published on Web 04/11/2006

enzyme clusters with animal α-fucosidases according to the phylogenetic tree analysis.

Recently, we established a rapid synthesis by amide-forming reactions in microtiter plates for high-throughput screening *in situ* without protecting group manipulation and product isolation, which identified potent and selective inhibitors against the α-fucosidases from *Corynebacterium* sp. and bovine kidney (*27*, *28*). This approach is based on a rapid screening for an optimal aglycon attached to the fuconojirimycin (FNJ)-based structure that mimics the transition state of enzymatic glycoside cleavage (*27*). The introduction of a hydrophobic moiety into the iminocyclitol core resulted in time-dependent inhibition; therefore, the inhibitory potency was greatly enhanced from a low nanomolar K_i to a picomolar K_i* value, leading to the discovery of the most potent glycosidase inhibitor to date (*28*). To take a close look at the two similar α-fucosidases, TmF and HuF, more than 240 FNJ-derived molecules were prepared by diversity-oriented synthesis to contain substitution or modification at C1, C2, C6, or N. The incubation of most C1-substituted FNJs with TmF was found to give a type of inhibition different from that with HuF. Slow and tight-binding inhibition was observed in the study of the former enzyme, which was distinct from the reversible inhibition of the latter. These molecules thus had a higher affinity for the bacterial α-fucosidase than the human enzyme. The best inhibitor exhibited a drastic difference of up to several thousand-fold mainly due to the extra hydrophobic binding site of TmF, as suggested by the structural information. To decipher the interesting distinction at a molecular level, we provide supporting evidence with site-directed mutagenesis, the comparison of inhibition constants among the wild-type and mutant proteins, and the intrinsic fluorescence change upon inhibitor titration.

EXPERIMENTAL PROCEDURES

Preparation of the α-Fucosidases from T. maritima and Human. The cloning, protein expression, and purification steps of the *Thermotoga* α-fucosidase were slightly modified from the procedures reported by Henrissat and Withers et al. (*26*, *29*). The pET21b expression vector encodes a C-terminal His_6 tag fused to the entire coding region of α-fucosidase. Sequence analysis indicated no difference from GenBank accession number NC_000853. The pCMV vector (purchased from Stratagene Co.) harboring the human α-fucosidase gene (GenBank accession number BC017338) was amplified and constructed in a pET22b system for protein expression. The 66 nucleotides at the 5′-end, corresponding to the 22 N-terminal amino acid residues as the signal peptide sequence, were deleted during the gene construction. The purification of the recombinant enzyme (HuF) involved the use of ammonium sulfate fractionation and two columns of ion-exchange chromatography. HuF was obtained with high purity (>95% homogeneity) on the basis of SDS−PAGE analysis. The detailed information, including gene construction, protein overexpression, and characterization, will be reported elsewhere.

Site-Directed Mutagenesis. The W58A, F59A, Y64A, L191A, M225A, and Y267A mutants were obtained by using the QuikChange mutagenesis kit (Stratagene Co.) in accordance with the manufacturer's instructions. The 5′-AGTGC CGATG GATGC CGCAT TCTTC CAGAA TCCGT ACG-3′ (sense) and 5′-CGTAC GGATT CTGGA AGAAT GCGGC ATCCA TCGGC ACT-3′ (antisense) primers were used to incorporate the mutation site of W58A. The 5′-GCCGA TGGAT GCCTG GGCAT TCCAG AATCC GTACG CAG-3′ (sense) and 5′-CTGCG TACGG ATTCT GGAAT GCCCA GGCAT CCATC GGC-3′ (antisense) primers were used to incorporate the mutation site of F59A. The 5′-TGGTT CTTCC AGAAT CCGGC AGCAG AGTGG TACGA AAATT CC-3′ (sense) and 5′-GGAAT TTTCG TACCA CTCTG CTGCC GGATT CTGGA AGAAC CA-3′ (antisense) primers were used to incorporate the mutation site of Y64A. The 5′-CCGAT AAGAT ACCCC GAGGA TGCAT CCTAC ATCAG GCCG-3′ (sense) and 5′-CGGCC TGATG TAGGA TGCAT CCTCG GGGTA TCTTA TCGG-3′ (antisense) primers were used to incorporate the mutation site of L191A. The 5′-GTTCT CTGGA ACGAC GCAGG CTGGC CGGAG AAAG-3′ (sense) and 5′-CTTTC TCCGG CCAGC CTGCG TCGTT CCAGA GAAC-3′ (antisense) primers were used to incorporate the mutation site of M225A. The 5′-GATTT CAAAA CGGCC GAGGC ACACG TGAAC TATCC GGG-3′ (sense) and 5′-CCCGG ATAGT TCACG TGTGC CTCGG CCGTT TTGAA ATC-3′ (antisense) primers were used to incorporate the mutation site of Y267A. The results were verified by DNA sequencing analysis. The mutant proteins were expressed and purified under the conditions described previously (*26*, *29*). Further confirmation was carried out by mass spectrometric analysis to see if the desired molecular weight is obtained.

*Rapid Synthesis of Compound **1**-, **2**-, and **3**-Derived FNJs in Microplates, Followed by an In Situ Inhibition Assay of α-Fucosidase*. The synthesis of amide derivatives in microplates was carried out as described previously (*27*, *28*). Assay mixtures (200 μL) contained 50 mM Hepes (pH 8.0), 0.1% BSA (by weight), 50 μM 4-methylumbelliferyl-α-L-fucopyranoside, and inhibitor (final concentrations of 1.0−3.0 nM). The α-fucosidase (0.2 nM) was added to initiate inhibition assays. The emission at 465 nm was monitored using an excitation wavelength of 360 nm to measure the release of fluorescent 4-methylumbelliferone at 20 °C.

In the case of time-dependent inhibition, the data were analyzed and determined to follow the aforementioned slow-binding inhibition pattern (eq 1).

$$E + I \underset{k_4}{\overset{k_3}{\rightleftharpoons}} E{\cdot}I \underset{k_6}{\overset{k_5}{\rightleftharpoons}} E{\cdot}I^* \qquad (1)$$

K_i spans $E + I \rightleftharpoons E{\cdot}I$; K_i^* spans $E + I \rightleftharpoons E{\cdot}I^*$

The kinetics can be described according to an integrated equation (eq 2)

$$P = v_s t + (v_0 - v_s)\frac{1 - e^{-kt}}{k} \qquad (2)$$

where v_0 and v_s are the initial and steady-state rates, respectively, k is the apparent rate constant for establishing the steady-state equilibrium, and P is the amount of product that accumulates during a period of time t.

In the case of slow tight-binding inhibition, the concentration of the E·I complex is not negligible in comparison with

the inhibitor concentration and the free inhibitor concentration is not equal to the added concentration of the inhibitor. Corrections have to be made for the reductions in the inhibitor concentration that occur upon formation of the E·I complex. The variation of the steady-state velocity with inhibitor concentration is given by the equations

$$v_s = \frac{k_7[S]Q}{2(K_m + [S])} \quad (3)$$

$$Q = \sqrt{(K_i' + [I]_t - [E]_t)^2 + 4K_i'[E]_t} - (K_i' + [I]_t - [E]_t) \quad (4)$$

where $K_i' = K_i(1 + [S]/K_m)$, k_7 is the rate constant for the product formation, and $[I]_t$ and $[E]_t$ stand for total inhibitor and enzyme concentrations, respectively. The relationship between the rate constant of enzymatic reaction k and the interconversion of the E·I and E·I* complexes can be expressed as eq 5.

$$k = k_6 + k_5\left(\frac{[I]/K_i}{1 + [S]/K_m + [I]/K_i}\right) \quad (5)$$

The progress curves were analyzed via eqs 2 and 5 using nonlinear least-squares parameter minimization to determine the best-fit values with the corrections for the tight-binding inhibition; i.e., the data were transferred into KaleidaGraph and fitted by the aforementioned equations.

Fluorescence Analysis of the Enzyme−Inhibitor Complex. The change of α-fucosidase intrinsic fluorescence upon addition of compound **8** was monitored using an F-4500 fluorescence spectrometer (Hitachi Co.). The emission spectra were recorded from 300 to 450 nm upon excitation of α-fucosidase at 285 nm. The fluorescence spectra of 0.44 μM α-fucosidase in 50 mM Hepes buffer (pH 8.0) at 20 °C were measured before and after addition of compound **8**.

RESULTS AND DISCUSSION

α-Fucosidases are found exclusively in family GH29 of the classification of glycosidases on the basis of sequence similarities, reflecting the folds, active site architecture, and molecular mechanism (*30*). This family of enzymes was demonstrated to follow a double-displacement mechanism with net retention of the anomeric configuration (*31*, *32*). According to the analysis of sequence alignment, the sequences of both TmF and HuF are 38% identical and 56% similar. Recently, Bourne and Henrissat et al. determined the crystal structure of TmF, as well as the structures of an enzyme−product complex and of a covalent glycosyl−enzyme intermediate (*26*). On the basis of the structural information, multiple-sequence alignment of TmF and HuF with the α-fucosidases from other species indicated that both enzymes could be aligned well with a high degree of sequence similarity according to the eight-element fingerprints of GH29, which was further supported by the secondary structure prediction. On the basis of the alignment, many functional amino acid residues are well-conserved, including the catalytic nucleophile, the general acid/base (*29*), the residues involved in the hydrogen bonding network with the fucose ring, and those for the hydrophobic contact with the C6 methyl group. The consistence allows the homology

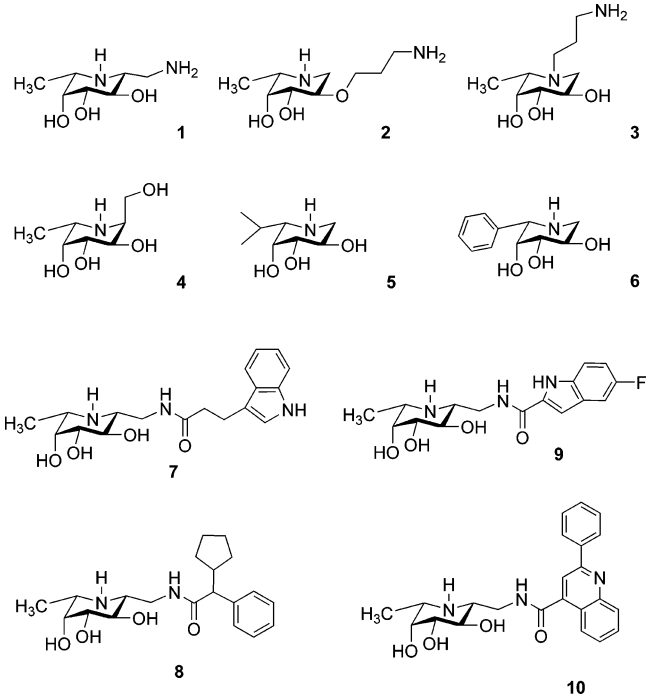

FIGURE 1: Molecular structures of compounds **1**−**10**.

modeling of the human α-fucosidase in accordance with the crystal structure of the TmF−inhibitor complex (PDB entry 1h19) (*26*). Residues 46−65 of TmF, being near the active site, are proposed to be essential for the major difference in the binding site between the two α-fucosidases, which also accounts for the different substrate specificity (*26*). The human enzyme lacks this additional sequence. It would be intriguing to distinguish the two enzymes by the use of inhibitors if the binding interactions are exclusive for one enzyme but not for the other.

To study the binding site difference, several FNJ derivatives or analogues, **1**−**6** (Figure 1), were prepared (*33*−*36*). The detailed synthetic procedures and characterization of all products will be published elsewhere. Their structures and IC_{50} values are given in Table 1. The inhibition activity was determined by measuring the remaining enzyme activity according to the fluorescence emission of 4-methylumbelliferone at 465 nm in the presence of 4-methylumbelliferyl-α-L-fucopyranoside (or *p*-nitrophenyl at 405 nm in the existence of *p*-nitrophenyl-α-L-fucopyranoside) (*27*, *28*). Every molecule gave a similar inhibition potency toward both α-fucosidases. In agreement with the previous study (*36*), the stereochemical configuration at C1 did not affect the enzyme inhibition, whereas the potency was diminished to a great degree by the modification at C6. In comparison with the C1 substitutions, the affinity was found to be slightly lower when an extra linker was introduced at C2 or the ring nitrogen.

Although the previous study identified no difference between the two α-fucosidases, the molecules produced by diversity-oriented synthesis led to an interesting discovery. The amide-forming reactions of compounds **1**−**3** with various acids were carried out in the presence of (1*H*-benzotriazol-1-yl)-1,1,3,3-tetramethyluronium hexafluorophosphate (HBTU, 1 equiv) and diisopropyl ethylamine (DIEA, 2 equiv) in wells of microtiter plates (Figure 2). Without product purification, the reaction mixtures were

Table 1: IC_{50} Values of Compounds **1**−**6** against the α-Fucosidases from *T. maritima* (designated TmF) and Human (HuF)[a]

	IC_{50} (nM)					
enzyme	**1**	**2**	**3**	**4**	**5**	**6**
TmF	64 ± 8.0	267 ± 19	70 ± 11	52 ± 2.8	6000 ± 500	7000 ± 300
HuF	35 ± 4.2	106 ± 13	92 ± 9.0	18 ± 1.2	3500 ± 300	2000 ± 180

[a] Assay condition: 50 mM Hepes (pH 8.0) containing 50 μM 4-methylumbelliferyl-α-L-fucopyranoside, inhibitor (1.0−3.0 nM), and α-fucosidase (0.2 nM). The enzyme was added to initiate the reaction assay.

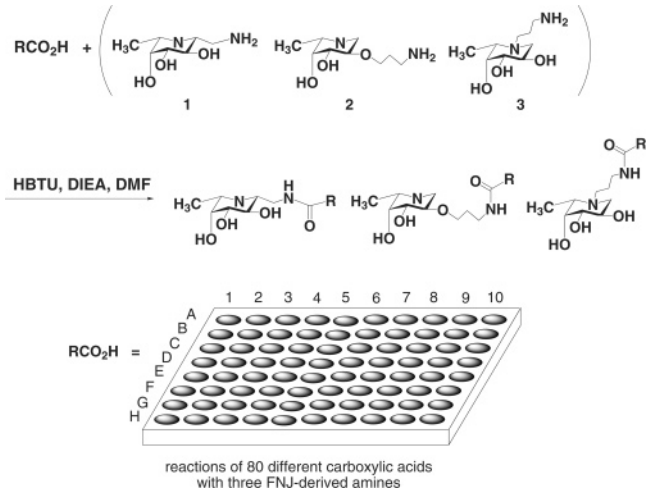

FIGURE 2: Reactions of FNJs **1**−**3** with a group of 80 carboxylic acids in microtiter plates for direct screening of α-fucosidase inhibition in situ. See the Supporting Information for the molecular structures of the carboxylic acids.

directly subjected to aqueous dilution and a screening assay for the inhibition against TmF and HuF. All the carboxylic acids alone did not exhibit any significant inhibition without amide bond formation. The reagents used in the coupling reactions (HBTU and DIEA) or the intermediate *N*-hydroxybenzotriazole (HOBT) also exhibited little inhibition. No significant inhibition was found against α- and β-glucosidase, α- and β-galactosidase, or α- and β-mannosidase (*27*).

For the purpose of an easy understanding and quick comparison, the potency was expressed as % inhibition at one concentration of the reaction products. Of the 240 molecules generated by the synthesis (Figure 2), C1-substituted FNJs were generally more potent than the others (**2**- and **3**-derived products) and the reactant amine (**1**). More than 80% of the coupling products of **1** were shown to exhibit enhanced inhibition against both α-fucosidases. On the other hand, only few coupling reactions of **2** and **3** resulted in an increase in inhibitory potency. Furthermore, compound **1**-derived molecules revealed dissimilar inhibition profiles toward both α-fucosidases; i.e., the favorable structures identified by fast screening of each α-fucosidase were not completely identical. As shown in Figure 3, the amide-forming reactions of **1** with A8, C5, F5, and G9 were among the best inhibitors of both α-fucosidases. The reaction products of D8, E9, and F8 were solely potent to the inhibition of TmF, while those of E8 and G5 only effectively inhibit the HuF activity (see the Supporting Information for the molecular structures of these acids). A more dramatic discrepancy was clearly manifested by the prolonged observation of enzyme inhibition assays. Most members of the compound **1**-based library displayed a time-dependent decrease in the reaction rates of the bacterial enzyme as a function of the inhibitor concentration (Figure 4A), indicating

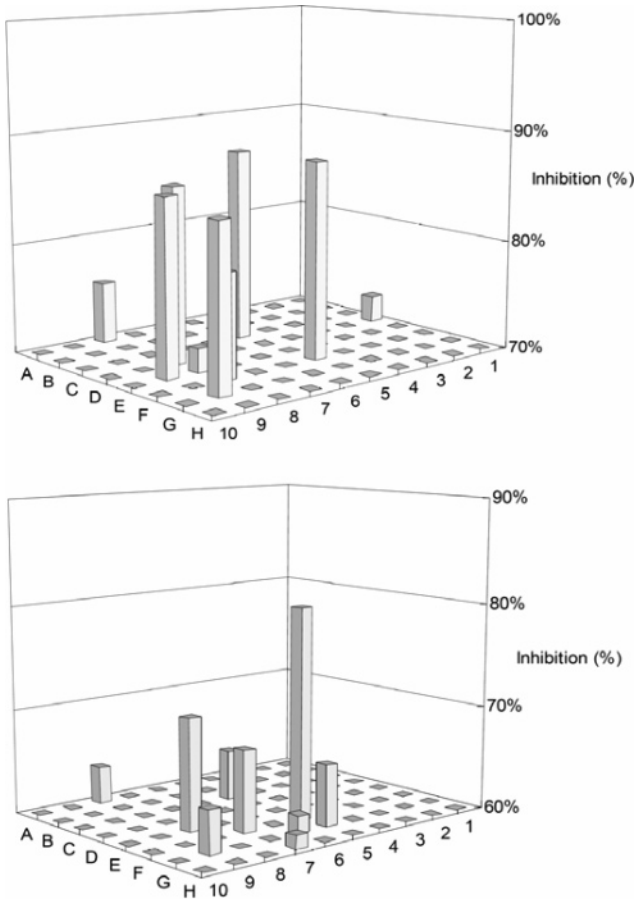

FIGURE 3: Different inhibition profiles shown by the fast screening of TmF (top) and HuF (bottom) with compound **1**-derived FNJs at 125 nM.

time-dependent, slow tight-binding inhibition. In sharp contrast, the same pool of molecules all demonstrated reversible inhibition against HuF (Figure 4B).

Analysis of the time-dependent progress curves of the TmF inhibition supported a two-step mechanism in which an initial collisional complex (E·I) is isomerized to a tighter complex (E·I*) (eq 1), in agreement with the previous report (*28*). The majority of compound **1**-derived inhibitors produced a progressive tightening of inhibition with linear initial rates followed by a gradual loss of activity. The inhibition constants K_i and K_i* were determined by fitting the observed data to the model. To clearly explain the different types of inhibition at a structural level, the previously synthesized inhibitors **7** (the coupling product of D8), **8** (product of E2), **9** (product of D5), and **10** (product of B3) were investigated in detail (see Figure 1 for the molecular structures of **7**−**10**). Table 2 lists the inhibition constants. Compound **7** is the most potent inhibitor whose binding affinity with TmF (K_i* = 0.41 pM) is significantly higher than that with HuF (K_i = 5.6 nM) up to 13700-fold. Furthermore, compound **1** is a

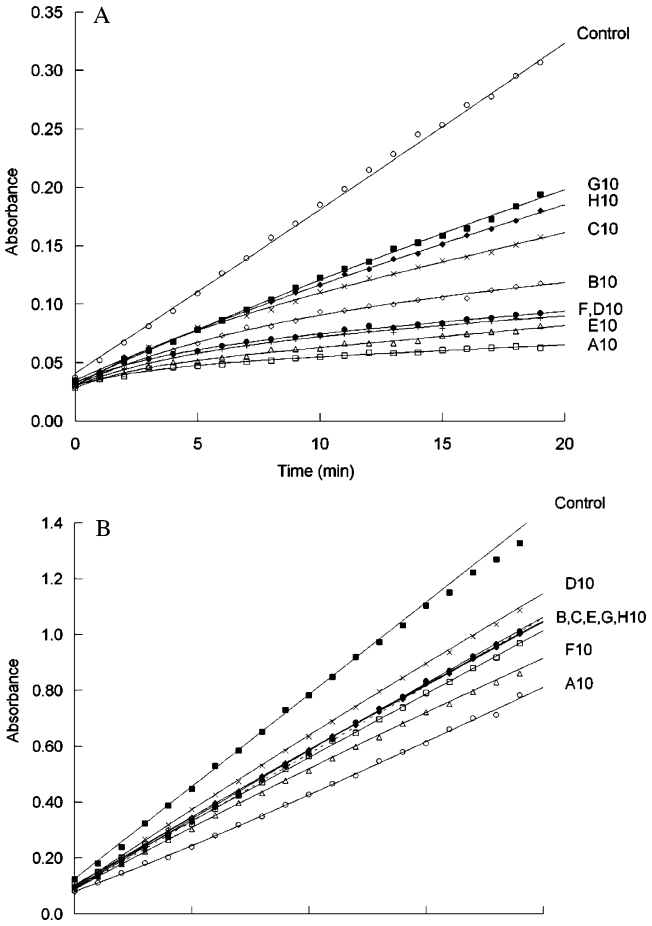

FIGURE 4: Progressive curves for the inhibition of (A) TmF and (B) HuF by the amide-forming reaction products (125 nM) of compound **1** with various carboxylic acids. For the purpose of clear presentation, only the coupling products of A10-G10 are shown.

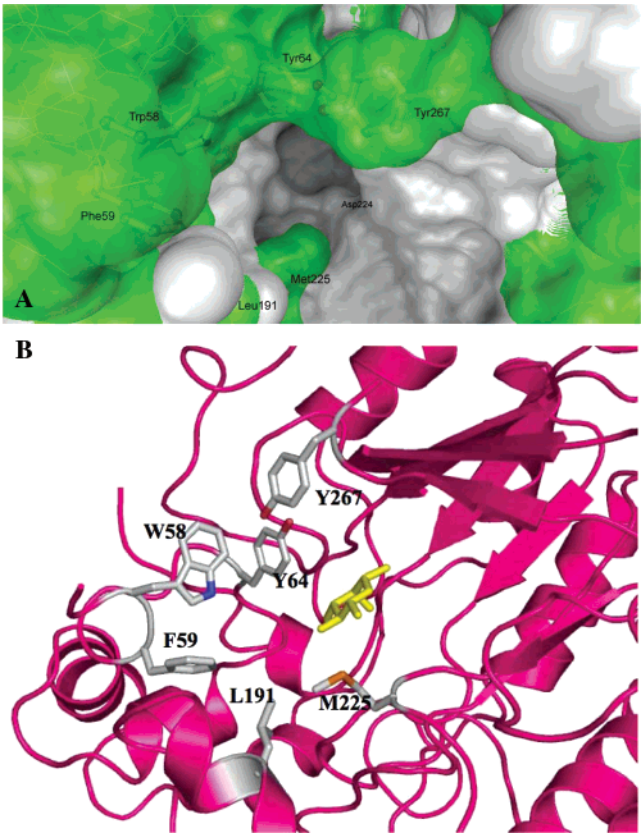

FIGURE 5: (A) Overlaid molecular surfaces of TmF (green) and HuF (white). The former was obtained from the reported X-ray crystal structure, and the latter is based on computational modeling. In the center, a deep hole represents the active site (Asp224 is the catalytic nucleophile). Trp58, Phe59, Tyr64, Leu191, Met225, and Tyr267 of TmF are located near the entrance of the active site and thus are proposed to interact with the aglycon of inhibitors. (B) Proposed residues of TmF to enhance the inhibitory potency. This is another view of the aforementioned X-ray crystal structure with bound 2-deoxy-2-fluorofucopyranose (yellow). The Cα side chains of the six proposed residues are displayed to indicate their proximity to the enzyme active site.

reversible inhibitor of TmF and HuF with K_i values of 6.8 and 15.2 nM, respectively. The introduction of aglycon D8 thus generated 1.7×10^4- and 2.7-fold enhancement of the inhibition potency toward TmF and HuF, respectively. As a consequence, these results strongly support the idea that both α-fucosidases have different binding sites to interact with the aglycon. It is also noteworthy that both TmF and HuF exhibit a pH dependence of catalysis and of inhibition, in agreement with the reports by Davies and co-workers (*37*−*39*). The preliminary result on a number of inhibitors (such as **1**, **8**, and **10**) indicated that the inhibitory species are protonated inhibitors bound to TmF whose acid/base and nucleophile are ionized at the studied pH of 8.0. The determination of whether the pH-dependent inhibition correlates with the presence of an extra proton donor or acceptor in a molecule is currently in progress and will be published elsewhere.

To identify the critical residues involved in the enhanced affinity, the modeling structure proposes that Trp58, Phe59, and Tyr64 of TmF, located in the aforementioned additional sequence of residues 46−65, likely play an important role by lining up to face the active site (Figure 5). Tyr267 is close to the three residues spatially and joins them to form a hydrophobic domain. Moreover, Leu191 and Met225 of TmF are worth attention because they are also in the proximity of the active site, and the human enzyme presents dissimilar groups at the corresponding positions (i.e., Leu191 of TmF is related to K193 of HuF and Met225 of TmF to G226 of HuF).

Each proposed residue in TmF was individually altered to alanine by site-directed mutagenesis. The mutant enzymes were prepared and purified according to the reported procedure of the wild-type protein (*29*). The mutation sites were verified by DNA sequencing, and each mutant protein

Table 2: Inhibition Constants (nM) of Compounds **1** and **7**−**10** against TmF and HuF[a]

	1	**7**		**8**		**9**		**10**	
enzyme	K_i	K_i	K_i*	K_i	K_i*	K_i	K_i*	K_i	K_i*
TmF	6.8 ± 1.1	0.105 ± 0.011	0.000409 ± 0.000044	1.01 ± 0.09	0.054 ± 0.002	0.259 ± 0.010	0.063 ± 0.002	1.19 ± 0.06	0.563 ± 0.028
HuF	15.2 ± 1.5	5.6 ± 0.2	−	18.0 ± 0.2	-	9.7 ± 0.3	−	11.7 ± 1.9	−

[a] Assay condition: 50 mM Hepes (pH 8.0) containing 50 μM 4-methylumbelliferyl-α-L-fucopyranoside, inhibitor (1.0−3.0 nM), and α-fucosidase (0.2 nM). The enzyme was added to initiate the reaction assay.

Table 3: Inhibition Constants (nM) of Compounds **1**, **7**, and **8** against the Wild Type and Five Mutant Proteins of TmF[a]

	1	**7**		**8**	
TmF	K_i	K_i	K_i*	K_i	K_i*
wild type	6.8 ± 1.1	0.105 ± 0.011	0.000409 ± 0.000044	1.01 ± 0.09	0.054 ± 0.002
F59A	12.8 ± 1.5	0.121 ± 0.022	0.0132 ± 0.0015	1.8 ± 0.3	0.17 ± 0.02
Y64A	9.4 ± 1.8	0.563 ± 0.072	−	5.8 ± 0.8	−
L191A	6.9 ± 0.7	0.113 ± 0.017	0.0071 ± 0.0005	1.2 ± 0.1	0.063 ± 0.006
M225A	6.8 ± 0.8	0.124 ± 0.015	0.0092 ± 0.0011	0.98 ± 0.16	0.094 ± 0.016
Y267A	10.9 ± 1.5	0.982 ± 0.120	−	6.3 ± 0.7	−

[a] Assay condition: 50 mM Hepes (pH 8.0) containing 50 μM 4-methylumbelliferyl-α-L-fucopyranoside, inhibitor (1.0−3.0 nM), and α-fucosidase (0.2 nM). The enzyme was added to initiate the reaction assay.

was subjected to mass spectrometry analysis to confirm the expected molecular weight. With the assay using 4-methylumbelliferyl-α-L-fucopyranoside, the two TmF mutants (Y64A and Y267A) behaved in a manner similar to that of the human enzyme in the progressive curves for the inhibition of compound **1**-derived FNJs; i.e., the rates of inhibition did not deviate from linearity, in contrast to the slow tight-binding inhibition of wild-type TmF. The preparation of mutant W58A was unsuccessful because of its instability. Slow tight-binding inhibition was still observed when the other F59A, L191A, and M225A mutants were individually incubated with the C1-substituted FNJs (Table 3). The kinetics of the latter two proteins were mostly like those of the wild type, whereas the potency of mutant F59A is between that of the wild type and that of both mutants Y64A and Y267A (i.e., the order of potency is wild type > F59A > Y64A ≈ Y267A). Meanwhile, except for W58A, the five stable mutant enzymes all retained an affinity for compound **1** comparable to the wild-type level, as shown by the K_i values in Table 3, indicating that the mutated residues have nothing to do with the sugar binding. On the other hand, compound **7** generated a huge difference in affinity between the wild type (K_i* = 0.41 pM) and the two mutants, Y64A (K_i = 0.56 nM) and Y267A (K_i = 0.98 nM), implying that the aforementioned enhanced affinity was reduced to a great extent because of such a specific mutation. Tyr64 and Tyr267 thus play indispensable roles in interacting well with the aglycon to significantly facilitate binding.

Additionally, the binding of compound **7** with the two mutants, Y64A and Y267A (K_i = 0.56 and 0.98 nM, respectively), appears to be tighter than that of **8** (K_i = 5.8 for Y64A and K_i = 6.3 nM for Y267A). Coincidently, the latter affinity is similar to that for the binding of the wild-type TmF with compound **1** (K_i = 6.8 nM). The aglycon of **7** obviously has a better fit to the indicated aglycon binding site. The statement was strengthened by a general trend in Table 3 which shows that inhibitor **7** has an ∼10 times higher affinity than **8** no matter whether the enzyme is the wild type or any mutant. The preliminary study of the molecular docking experiments revealed that compound **7**, containing two methylene units between the amide and indole group, apparently has more flexibility to allow better adjustment and fit for a tighter binding, unlike more restricted conformations in compounds **8**−**10**. Meanwhile, the indole nitrogen of compound **7** is found to have an additional hydrogen bonding with the phenol of Y267 (also possibly with that of Y64).

In our previous report, the slow tight-binding inhibition was suggested to result from the protein conformational change induced by the hydrophobic aglycon, as supported by the concentration-dependent and time-dependent fluorescence increase upon inhibitor titration (*30*). The fluorescence emission spectra of TmF displayed an emission maximum (λ_{max}) at 336 nm in the presence and absence of compound **8** as a consequence of the radiative enhancement of the $\pi-\pi^*$ transition from the tryptophan residues. The inhibitor binding led to a concentration-dependent increase in the fluorescence with an utmost enhancement of 50% (Figure 6A). Replacement of the inhibitor with compound **1** led to no increase in fluorescence, indicating that the enhancement corresponds to aglycon binding. On the other hand, the fluorescence of mutant Y267A did not change with the inhibitor titration of compound **8** (Figure 6B), neither did the fluorescence study of mutant Y64A (Figure 6C). Mutant F59A has a moderate increase of ∼25%, compared with 45−50% enhanced fluorescence in the study of L191A and M225A. These results not only echo the aforementioned kinetic data but also corroborate the important contribution of Y64 and Y267 to enhanced binding. Interestingly, the intrinsic fluorescence of HuF did not produce any change upon inhibitor titration (data not shown).

Furthermore, it is intriguing that only C1-substituted FNJs achieved good inhibition, rather than C2- and N-derived FNJ analogues. Examination of the crystal structure of TmF in complex with L-fucose (the reaction product) revealed that the sugar residue is compactly surrounded by the enzyme with each functional group interacting with one or more protein side chains. One exception is the entrance of the active site, which is near the hydroxyl group of C2. Bourne and co-workers (*26*) presented this feature to account for the biological role of α-fucosidases in the capable digestion of branched glycans. However, why do C1-substututed FNJs, instead of C2-derived FNJs, demonstrate enhanced binding with TmF? Our preliminary result of the modeling studies of TmF with a series of C1-derived FNJs suggests that, in comparison with the TmF−L-fucose structure, the iminocyclitol ring rotates 24° to move the ring nitrogen (likely exiting as a protonated form) to have additional electrostatic interactions with Asp224 and Glu266. Such subtle movement makes better accommodation for C1-extended FNJs, rather than the FNJs with a substitution at other positions.

The work provides several pieces of evidence to support the importance of Y64 and Y267 in the extra binding interactions, leading to the great enhancement of inhibition potency against TmF. As a matter of fact, a number of reports have offered a similar view that the binding of a small molecule could induce conformational change in a certain local structure (a flexible loop found in most cases) in the corresponding enzyme, such as triclosan to bind with acyl-carrier protein reductase (or enoyl-ACP reductase) (*40*, *41*),

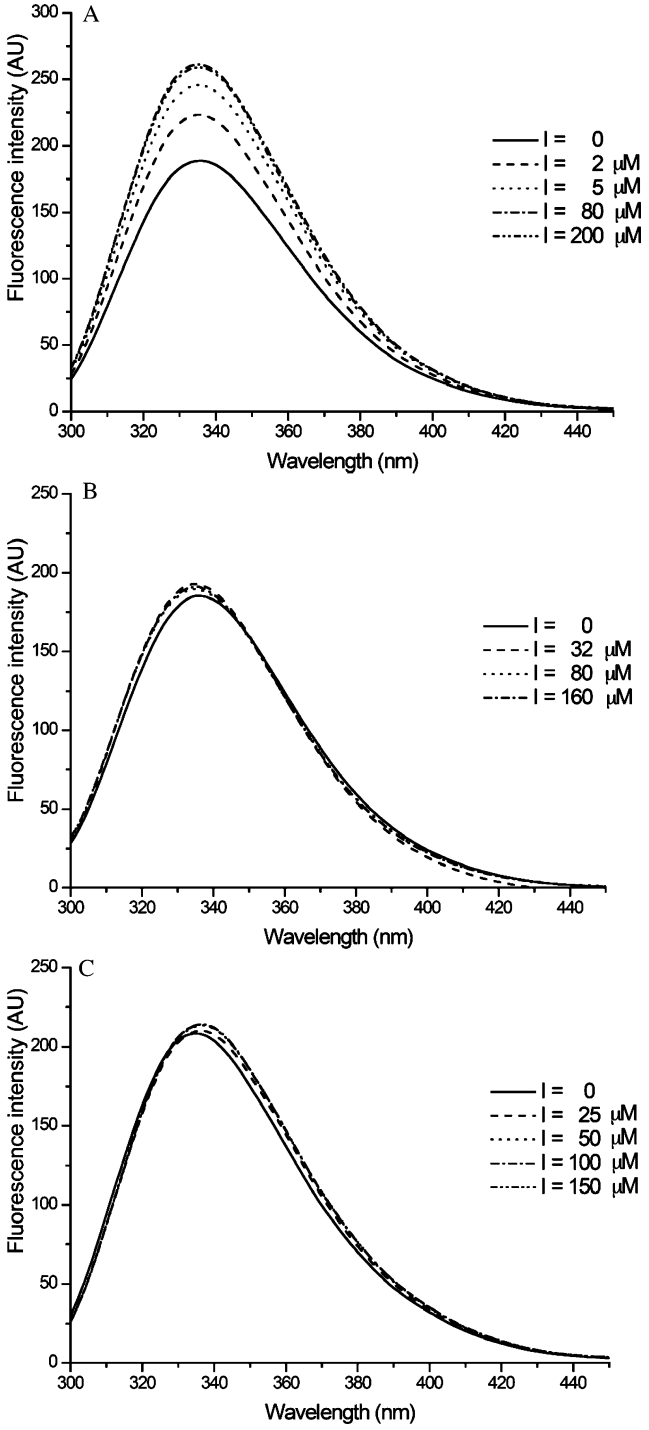

FIGURE 6: Fluorescence emission spectra. (A) Steady-state fluorescence emission spectra of TmF as a function of inhibitor **8** concentration. The study was carried out in the presence of 0.44 μM TmF in 50 mM Hepes (pH 8.0) at 20 °C. (B) Emission spectra of mutant Y267A under the same conditions as in panel A except for the protein. (C) Emission spectra of mutant Y64A under the same conditions as for panel A except for the protein.

fosmidomycin to bind with 1-deoxy-D-xylulose-5-phosphate reductoisomerase (DXR) (*42*), and inhibitors of cyclooxygenase (COX) (*43, 44*).

In conclusion, the diversity-oriented synthesis on the basis of a transition-state mimic is a powerful way to rapidly disclose small but significant differences in binding sites among similar enzymes, in addition to the fast discovery of potent and selective inhibitors. As a matter of fact, it is possible to distinguish more closely related α-fucosidases even by the limited number of members of our FNJ library. For example, the amide-forming reactions of compound **1** with A7 and F9 at a concentration of 125 nM were found to give 85 and 78% inhibition against TmF but 20 and 10% inhibition against the α-fucosidase from *Corynebacterium* sp., respectively. The reaction product of H9 with compound **1** also exhibited an apparent difference in the inhibition of the human and bovine kidney α-fucosidases. Therefore, this work provides a valuable platform for pinpointing selective inhibitors with less or no involvement of other related enzymes, as well as for helping to evaluate the specificity of developed molecules during drug discovery.

SUPPORTING INFORMATION AVAILABLE

Molecular structures of the 80 carboxylic acids, ^{1}H and ^{13}C NMR spectra of compounds **2**, **3**, and **5**−**10**, mass spectra of the mutant proteins, and fluorescence emission spectra of F59A and L191A. This material is available free of charge via the Internet at http://pubs.acs.org.

REFERENCES

1. Colegate, S. M., Huxtable, C. R., and Dorling, P. R. (1979) A spectroscopic investigation of swainsonine: An α-mannosidase inhibitor isolated from *Swainsona canescens*, *Aust. J. Chem. 32*, 2257−64.
2. Molyneux, R. J., and James, L. F. (1981) Loco intoxification: Indolizidine alkaloid of spotted locoweed, *Science 216*, 190−1.
3. Dorling, P. R., Huxtable, C. R., and Colegate, S. M. (1980) Inhibition of lysosomal α-mannosidase by swainsonine, an indolizidine alkaloid isolated from *Swainsona canescens*, *Biochem. J. 191*, 649−51.
4. Elbein, A. D., Solf, R., Dorling, P. R., and Vosbeck, K. (1981) Swainsonine: An inhibitor of glycoprotein processing, *Proc. Natl. Acad. Sci. U.S.A. 78*, 7393−7.
5. Dennis, J. W. (1986) Effects of swainsonine and polyinosinic-polycytidylic acid on murine tumor cell growth and metastasis, *Cancer Res. 46*, 5131−6.
6. Humphries, M. J., Matsumoto, K., White, S. L., and Olden, K. (1986) Oligosaccharide modification by Swainsonine treatment inhibits pulmonary colonization by B16-F10 murine melanoma cells, *Proc. Natl. Acad. Sci. U.S.A. 83*, 1752−6.
7. Tulsiani, D. R., Harris, T. M., and Touster, O. (1982) Swainsonine inhibits the biosynthesis of complex glycoproteins by inhibition of Golgi mannosidase II, *J. Biol. Chem. 257*, 7936−9.
8. De Gasperi, R., Daniel, P. F., and Warren, C. D. (1992) A human lysosomal α-mannosidase specific for the core of complex glycans, *J. Biol. Chem. 267*, 9706−12.
9. Gross, P. E., Reid, C. L., Bailey, D., and Dennis, J. W. (1997) Phase IB clinical trial of the oligosaccharide processing inhibitor swainsonine in patients with advanced malignancies, *Clin. Cancer Res. 3*, 1077−86.
10. Alderton, W. K., Cooper, C. E., and Knowles, R. G. (2001) Nitric oxide synthase: Structure, function and inhibition, *Biochem. J. 357*, 593−615.
11. Klibourn, R. G., and Griffith, O. W. (1992) Overproduction of nitric oxidein cytokine-mediated and septic shock, *J. Natl. Cancer Inst. 84*, 827−31.
12. Palmer, R. M. J. (1993) The discovery of nitric oxide in the vessel wall. A unifying concept in the pathogenesis of sepsis, *Arch. Surg. 128*, 396−401.
13. McCartney-Francis, N., Allen, J. N. Mizel, D. E., Albina, J., Xie, Q. W., Nathan, C. F., and Wahl, S. M. (1993) Suppression of arthritis by an inhibitor of nitric oxide synthase, *J. Exp. Med. 178*, 749−53.
14. Miller, M. J. S., Sadowska-Krowicka, H., Chotinaruenol, S., Kakkis, J. L., and Clark, D. A. (1993) Amelioration of chronic iletis by nitric oxidesynthase inhibition, *J. Pharmacol. Exp. Ther. 264*, 11−6.
15. Dawson, V. L., Dawson, T. M., London, E. D., Bredt, D. S., and Snyder, S. H. (1991) Nitric oxide mediates glutamate neurotoxicity in primary cortical cultures, *Proc. Natl. Acad. Sci. U.S.A. 88*, 6368−71.

16. Garthwaite, J. (1991) Glutamate, nitric oxide and cell−cell signaling in the nervous system, *Trends Neurosci. 14*, 60−7.
17. Moloney, D. J., Shair, L. H., Lu, F. M., Xia, J., Locke, R., Matta, K. L., and Haltiwanger, R. S. (2000) Mammalian Notch1 is modified with two unusual forms of O-linked glycosylation found on epidermal growth factor-like modules, *J. Biol. Chem. 275*, 9604−11.
18. Hooper, L. V., and Gordon, J. I. (2001) Glycans as legislators of host-microbial interactions: Spanning the spectrum from symbiosis to pathogenicity, *Glycobiology 11*, 1R−10R.
19. Hiraishi, K., Suzuki, K., Hakomori, S., and Adachi, M. (1993) Le(y) antigen expression is correlated with apoptosis (programmed cell death), *Glycobiology 3*, 381−90.
20. Lowe, J. B. (2002) Glycosylation in the control of selectin counter-receptor structure and function, *Immunol. Rev. 186*, 19−36.
21. Ayude, D., Fernandez-Rodriguez, J., Rodriguez-Berrocal, F. J., Martinez-Zorzano, V. S., de Carlos, A., Gil, E., and de La Cadena, M. P. (2000) Value of the serum α-L-fucosidase activity in the diagnosis of colorectal cancer, *Oncology 59*, 310−6.
22. Fernandez-Rodriguez, J., Ayude, D., de La Cadena, M. P., Martinez-Zorzano, V. S., de Carlos, A., Caride-Castro, A., de Castro, G., and Rodriguez-Berrocal, F. J. (2000) α-L-Fucosidase enzyme in the prediction of colorectal cancer patients at high risk of tumor recurrence, *Cancer Detect. Prev. 24*, 143−9.
23. Glick, M. C., Kothari, V. A., Liu, A., Stoykova, L. I., and Scanlin, T. F. (2001) Activity of fucosyltransferases and altered glycosylation in cystic fibrosis airway epithelial cells, *Biochimie 83*, 743−7.
24. Scanlin, T. F., and Glick, M. C. (1999) Terminal glycosylation in cystic fibrosis, *Biochim. Biophys. Acta 1455*, 241−53.
25. Giardina, M. G., Matarazzo, M., Morante, R., Lucariello, A., Varriale, A., Guardasole, V., and De Marco, G. (1998) Serum α-L-fucosidase activity and early detection of hepatocellular carcinoma: A prospective study of patients with cirrhosis, *Cancer 83*, 2468−74.
26. Sulzenbacher, G., Bignon, C., Nishimura, T., Tarling, C. A., Withers, S. G., Henrissat, B., and Bourne, Y. (2004) Crystal structure of *Thermotoga maritima* α-L-fucosidase, *J. Biol. Chem. 279*, 13119−28.
27. Wu, C.-Y., Chang, C.-F., Chen, J. S.-Y., Wong, C.-H., and Lin, C.-H. (2003) Rapid Diversity-Oriented Synthesis Followed by *In Situ* Screening: Identification as Potent and Selective α-Fucosidase Inhibitors, *Angew. Chem., Int. Ed. 42*, 4661−4.
28. Chang, C.-F., Ho, C.-W., Wu, C.-Y., Chao, T.-A., Wong, C.-H., and Lin, C.-H. (2004) Discovery of Picomolar Slow Tight-Binding Inhibitors of α-Fucosidase, *Chem. Biol. 11*, 1301−6.
29. Tarling, C. A., He, S., Sulzenbacher, G., Bignon, C., Bourne, Y., Henrissat, B., and Withers, S. G. (2003) Identification of the caalytic ncleophile of the fmily 29 α-L-fucosidase from *Thermotoga maritima* through trapping of a covalent glycosyl-enzyme intermediate and mutagene, *J. Biol. Chem. 278*, 47394−9.
30. Henrissat, B. (1991) A classification of glycosyl hydrolases based on amino acid sequence similarities, *Biochem. J. 280*, 309−16.
31. Berteau, O., McCort, I., Goasdoue, N., Tissot, B., and Daniel, R. (2002) Characterization of a new α-L-fucosidase isolated from the marine mollusk *Pecten maximus* that catalyzes the hydrolysis of α-L-fucose from algal fucoidan (*Ascophyllum nodosum*), *Glycobiology 12*, 272−82.
32. Cobucci-Ponzano, B., Trincone, A., Giordano, A., Rossi, M., and Moracci, M. (2003) Identification of an Archaeal α-L-fucosidase encoded by an interrupted gene, *J. Biol. Chem. 278*, 14622−31.
33. Fleet, G. W. J., Namgoong, S. K., Barker, C., Baines, S., Jacob, G. S., and Winchester, B. (1989) Iminoheptitols as glycosidase inhibitors: Synthesis of and specific α-L-fucosidase inhibition by β-L-homofuconojirimycin and 1-β-C-substituted deoxymannojirimycins, *Tetrahedron Lett. 30*, 4439−42.
34. Fleet, G. W. J., Ramsden, N. G., and Witty, D. R. (1989) Practical synthesis of deoxymannojirimycin and mannonolactam from L-gulonolactone: Synthesis of L-deoxymannojirimycin and L-mannonolactam from D-gulonolactone, *Tetrahedron 45*, 319−26.
35. Shilvock, J. P., and Fleet, G. W. J. (1998) The Synthesis of Deoxygalactostatin and 2,6-Imino-heptitol Derivatives via Stannane Mediated Hydroxymethylation of 5-Azido-1,4-lactones, *Synlett*, 554−6.
36. Fleet, G. W. J., Petursson, S., Campbell, A. L., Mueller, R. A., Behling, J. R., Babiak, K. A., Ng, J. S., and Scaros, M. G. (1989) Short Efficient Synthesis of the α-L-Fucosidase Inhibitor, Deoxyfuconojirimycin (1,5-Dideoxy-1,5-imino-L-fucitol), from D-Lyxonolactone, *J. Chem. Soc., Perkin Trans. 1*, 665−6.
37. Varrot, A., Tarling, C. A., Macdonald, J. M., Stick, R. V., Zechel, D. L., Withers, S. G., and Davies, G. J. (2003) Direct observation of the protonation state of an imino sugar glycosidase inhibitor upon binding, *J. Am. Chem. Soc. 125*, 7496−7.
38. Zechel, D. L., Boraston, A. B., Gloster, T., Boraston, C. M., Macdonald, J. M., Tilbrook, D. M., Stick, R. V., and Davies, G. J. (2003) Iminosugar glycosidase inhibitors: Structural and thermodynamic dissection of the binding of isofagomine and 1-deoxynojirimycin to β-glucosidases, *J. Am. Chem. Soc. 125*, 14313−23.
39. Gloster, T., Williams, S. J., Roberts, S., Tarling, C. A., Wicki, J., Withers, S. G., and Davies, G. J. (2004) Atomic resolution analysis of the binding of xylobiose-derived deoxynojirimycin and isofagomine to xylanase Xyn10A, *Chem. Commun.*, 1794−5.
40. Kapoor, M., Reddy, C. C., Krishnasastry, M. V., Surolia, N., and Surolia, A. (2004) Slow-tight-binding inhibition of enoyl-acyl carrier protein reductase from *Plasmodium falciparum* by triclosan, *Biochem. J. 381*, 719−24.
41. Levy, C. W., Roujeinikova, A., Sedelnikova, S., Baker, P. J., Stuitje, A. R., Slabas, A. R., Rice, D. W., and Rafferty, J. B. (1999) Molecular basis of triclosan activity, *Nature 398*, 383−4.
42. Yajima, S., Nonaka, T., Kuzuyama, T., Seto, H., and Ohsawa, K. (2002) Crystal structure of 1-deoxy-D-xylulose 5-phosphate reductoisomerase complexed with cofactors: Implications of a flexible loop movement upon substrate binding, *J. Biochem. 131*, 313−7.
43. Copeland, R. A., Williams, J. M., Giannaras, J., Nurnberg, S., Covington, M., Pinto, D., Pick, S., and Trzaskos, J. M. (1994) Mechanism of selective inhibition of the inducible isoform of prostaglandin G/H synthase, *Proc. Natl. Acad. Sci. U.S.A. 91*, 11202−6.
44. Gierse, J. K., McDonald, J. J., Hauser, S. D., Rangwala, S. H., Koboldt, C. M., and Seibert, K. (1996) A single amino acid difference between cyclooxygenase-1 (COX-1) and -2 (COX-2) reverses the selectivity of COX-2 specific inhibitors, *J. Biol. Chem. 271*, 15810−4.

BI052559N